

# A Parametric Study and Design Equation of Reinforced Concrete Deep Beams Subjected to Elevated Temperature



Hend S. Zayan, Jamal A. Farhan, Akram S. Mahmoud  
and Juma'a A. AL-Somaydaii

**Abstract** Reinforced concrete may be subjected to temperature due to climatic change or fire. However, deep beams can be exposed to various temperatures. This study will be treated and focused on the criteria of thermal analysis of deep beams. Many lectures are verified by nonlinear finite element method. Also, a parametric study is carried out to investigate the effect of some factors on the behavior of deep beams exposed to elevated temperature. The models are analyzed by the finite element method using (ANSYS) package. These factors are temperature, concrete compressive strength, and the shear span-to-effective depth ( $a/d$ ) ratio. The results show that when the temperature increases with constant compressive strength and ( $a/d$ ) ratio, the load capacity and deflection at failure are decreased, while when compressive strength increased, the load capacity and deflection at failure are increased for the same ( $a/d$ ) ratio and the same temperature. Finally, the results show that the load capacity decreases and deflection increases with an increase in ( $a/d$ ) ratio for the same temperature and same compressive strength. In addition to the parametric study, the proposed model to predict the strength of the deep beams exposed to high temperature is derived using artificial neural network by MATLAB and SPSS facilities. The error ( $R$ ) had been (0.99) and square value ( $R^2 = 0.98$ ). This means that the model is efficient and the error is very small.

**Keywords** Deep beams · Elevated temperature · ANSYS · Parametric study  
Artificial neural networks

## 1 Introduction

The deep beam is a beam when effective span-to-depth ratio ( $a/d$ ) is 4 or less as defined by ACI code [1, 2]. The Euro-International Concrete Committee defined deep beam if span length to hole depth ( $L/H$ )  $< 2$  for simply supported beam and

---

H. S. Zayan (✉) · J. A. Farhan · A. S. Mahmoud · J. A. AL-Somaydaii  
Civil Engineering Department, University of Anbar, Ramadi, Iraq  
e-mail: areesakhs@gmail.com

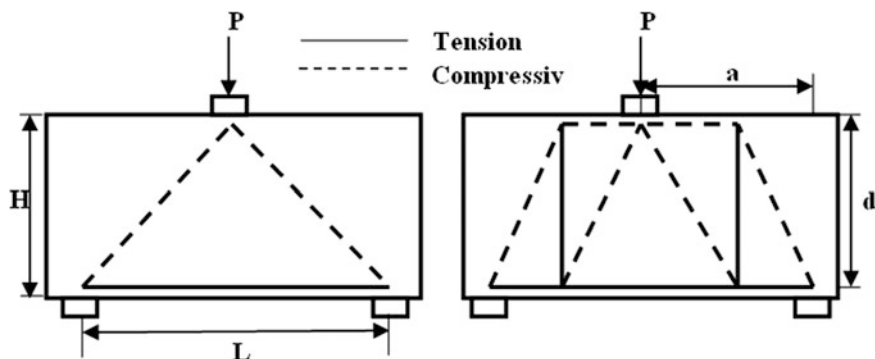


Fig. 1 Strut and Tie method details [5]

$(L/H) < 2.5$  for continuous beam [3], As shown in Fig. 1. Deep beam has various uses such as transfer deep girders, wall footing, foundation pile caps, bunkers, foundation beams, floor diaphragms, and shear walls. It fails usually by shear, there are two types of shear failure [4] (1-diagonal compression failure: occur nearly along the line joining the load point and the support point, 2-diagonal tension failure: occur by clean fracture near along the line joining support with the nearest loading point) as shown in Fig. 1.

High temperature has significant effects on behavior and strength of deep beams. When temperature increases, in ultimate load and failure deflection are clearly decreasing [6–8]. In this paper, the deep beam models were analyzed by finite element analysis using ANSYS package, then the parametric study was carried out for the models (i.e., some factors are changed with respect to others) where three different factors are varying. The first one is temperature ( $T$ ), and seven temperatures are considered (20, 100, 300, and 500) °C. The second factor is compressive strength ( $f'_c$ ), and five strengths are considered (30, 50, and 70) MPa. The third factor is load span-to-length ( $a/d$ ) ratio, and three values are considered (1, 2, and 3). One hundred and five (105) samples are investigated to evaluate these changes.

## 2 Modeling

The model dimensions were the width ( $b = 100$ ) mm, height ( $h = 225$ ) mm, and length varied as (750, 1150, and 1550) mm, for  $a/d$  ratios (1, 2, and 3) respectively. The concrete cover was (25) mm in all specimens. The reinforcement configurations are the same for all the samples as shown in Fig. 2. Tables 1 and 2 show the details of the analyzed samples. Their results showed clearly the deterioration in properties and ultimate load with high temperature. Theoretical model is adequate by comparing it with experimental works from the literature research [9].

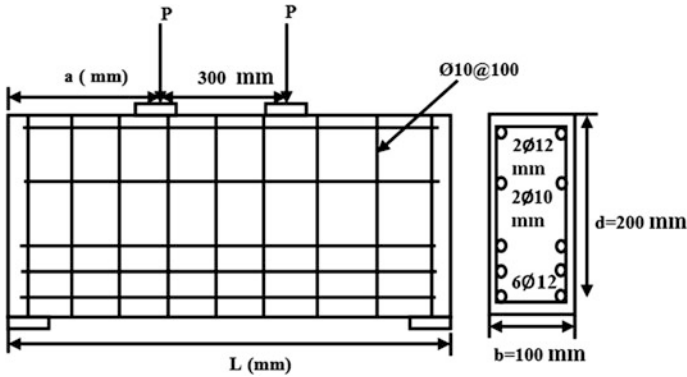


Fig. 2 Deep beam specimen details

Table 1 Sample properties

Structural component	Open shear transfer coefficient	Closed shear transfer coefficient	Compressive strength (MPa)	Yield stress (MPa)	Young's modulus (MPa)	Tangent modulus (MPa)	Area (mm <sup>2</sup> )
Symbols	$\beta_t$	$\beta_c$	$f'_c$	$f_y$	$E$	$E_T$	$BA$
Concrete	0.4	0.9	30	-	21,153	-	-
			50		30,836		
			70		39,574		
Steel reinforcement (Ø 12 mm)	-	-	-	838	195,150	19,515	113
Steel reinforcement (Ø 10 mm)	-	-	-	408	204,850	20,485	78.5

Table 2 Thermal properties of tested specimen

Structural component	Symbol	$T = 100\text{ }^\circ\text{C}$	$T = 300\text{ }^\circ\text{C}$	$T = 500\text{ }^\circ\text{C}$
Concrete	$K$	1.765	1.361	1.042
	$C$	900	1050	1100
	$\rho$	2331	2284	2237
Steel reinforcement	$K$	60	60	60
	$C$	500	500	500
	$\rho$	7850	7850	7850

### 3 Parametric Study of Elevated Temperature Effect

Seven stages in temperature are made in this study to evaluate the concrete behavior under different degrees of temperature for each compressive strength and ( $a/d$ ) ratio. These temperatures are (20, 100, 300, and 500) °C. From Figs. 3, 4, 5, 6, 7, 8, 9, 10, and 11, the results show that by increasing the temperature for the samples, the load capacity and deflection at failure are decreased. Each curve shows the load–deflection relation for constant compressive strength and ( $a/d$ ) ratio. Also, from these curves, it can be noticed that for  $a/d = 1$ , curves are not distinguished like curves with  $a/d = 3$ . That means with increasing length, deep beam samples will be more clear in the behavior [10, 11].

The sample of specimens included as DT (temp.  $a/d$ ), where DT means deep beam exposed to elevated temperature, (temp.) is the value of temperature (°C), (compressive strength of concrete (MPa), ( $a/d$ ) shear span-to-effect depth ratio. The mark (#) means various values of a parameter which is studied.

**Fig. 3** Load–deflection behavior for DT(#).30.1

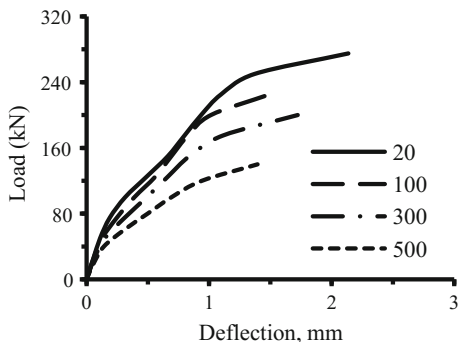


**Fig. 4** Load–deflection behavior for DT(#).30.2

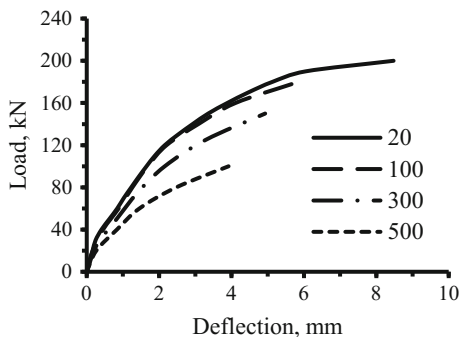


**Fig. 5** Load–deflection behavior for DT(#).30.3

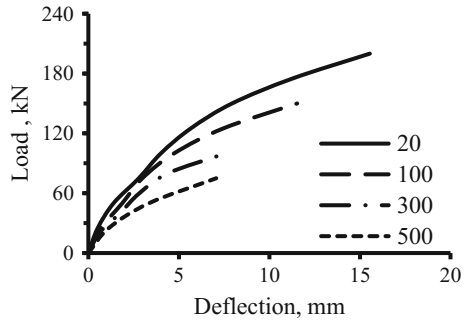


**Fig. 6** Load–deflection behavior for DT(#).50.1

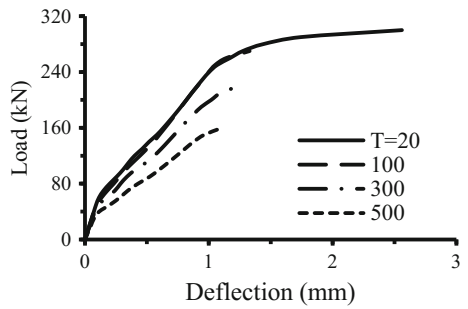
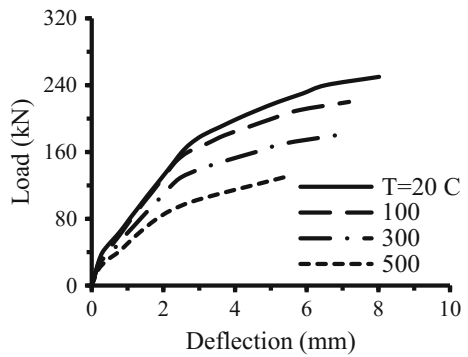


**Fig. 7** Load–deflection behavior for DT(#).50.2



For specimens having concrete compressive strength more than 40 MPa, the behavior of samples with  $a/d = 1$  will be more distinguished just like  $a/d = 2$  and  $a/d = 3$ . This means that for high-strength concrete, the effect of high temperature had less effect on concrete, not as for normal concrete.

**Fig. 8** Load–deflection behavior for DT(#).50.3

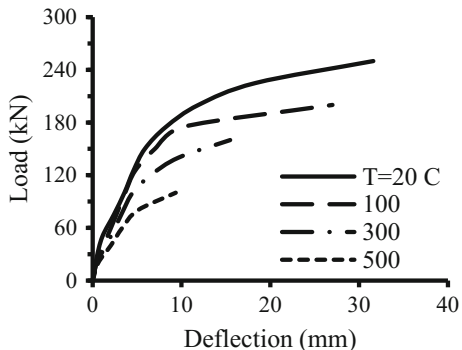


**Fig. 9** Load–deflection behavior for DT(#).70.1

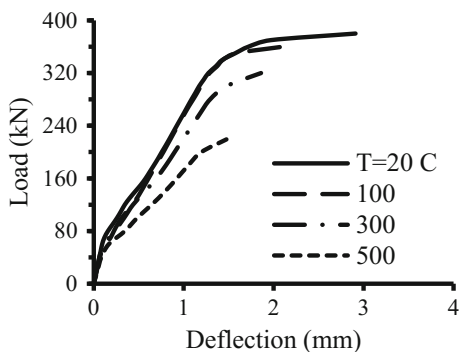


**Fig. 10** Load–deflection behavior for DT(#).70.2

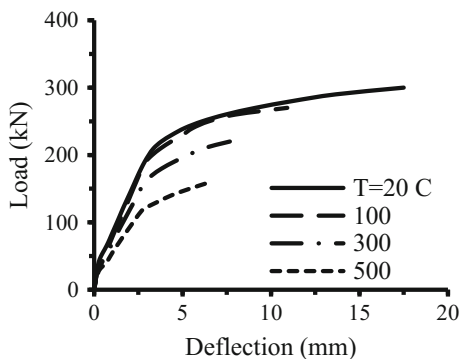
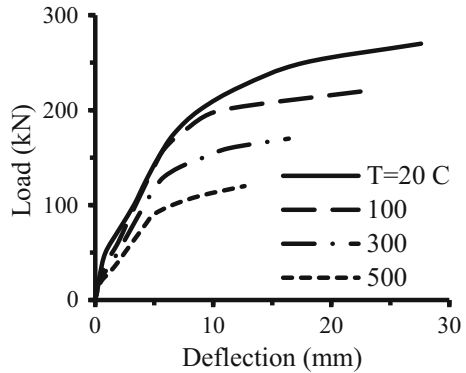


**Fig. 11** Load–deflection behavior for DT(#).70.3



### 4 Effect of Concrete Compressive Strength

In this study, five types of models are considered to evaluate the behavior of concrete with respect to different temperature strengths. The five strengths are (30, 50, and 70) MPa. They are selected to show the behavior of normal, moderate, and high-strength concrete. Figures 12, 13, 14, 15, 16, 17, 18, 19 and 20 show this behavior. The results show that by increasing the compressive strength for the samples, the load capacity and deflection at failure are increased with the same ( $a/d$ ) ratio and same temperature (Figs. 21, 22 and 23).

For ( $a/d = 1$ ) and temperature (20) °C, the increase of compressive strength about (3.5) times leads to an increase in ultimate load about (1.90) times. But for temperature (250) °C, the ultimate load increases to about (2.61) times. And for a temperature of (500) °C, the ultimate load increases to about (2.2) times.

That means by increasing the temperature, the percentage of ultimate load increases and then decreases as shown in Fig. 24. Because, at first, the water in the open voids is drying, so the disjoining pressure is going away and increase the strength of the concrete that leads to the increase in the ultimate load [8, 12–14]. Then with temperature raises, the water in closed voids is drying leading to thermal shrinkage and the strength decreases that reduces the ultimate load.

**Fig. 12** Load–deflection behavior for DT20.(#).1

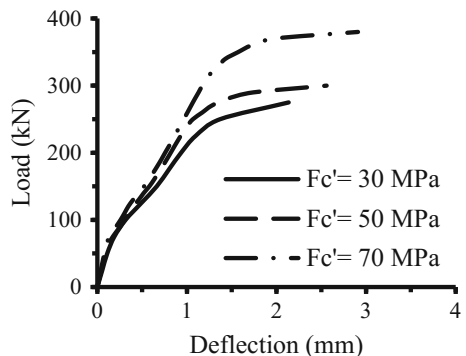


**Fig. 13** Load–deflection behavior for DT20.(#).2

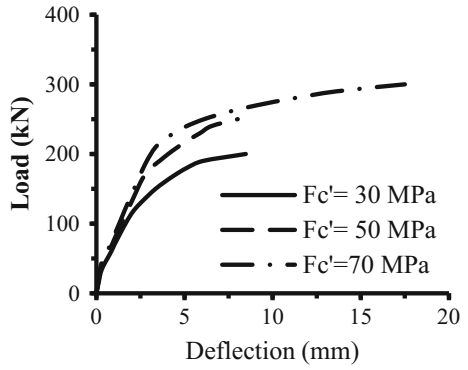


**Fig. 14** Load–deflection behavior for DT20.(#).3

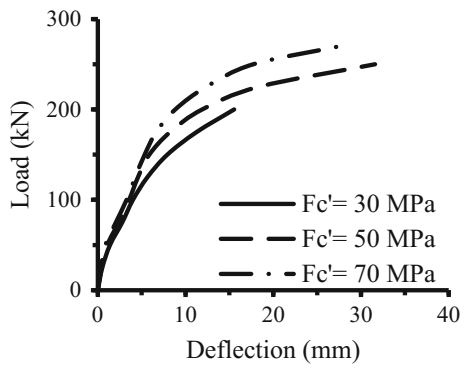


**Fig. 15** Load–deflection behavior for DT100.(#).1

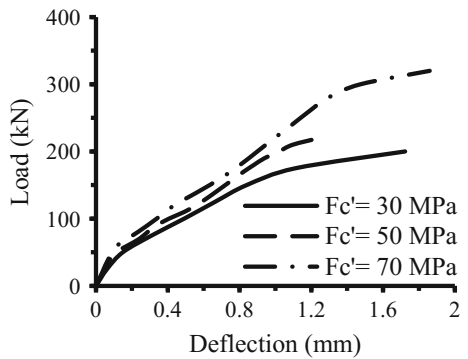




**Fig. 16** Load–deflection behavior for DT100.(#).2

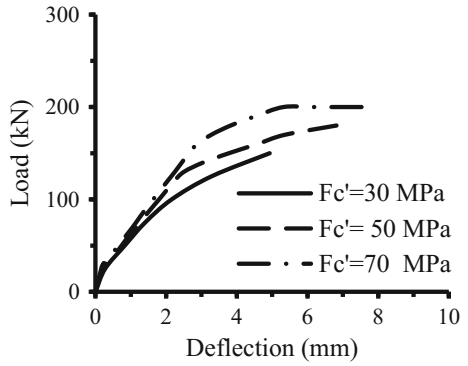


**Fig. 17** Load–deflection behavior for DT100.(#).3

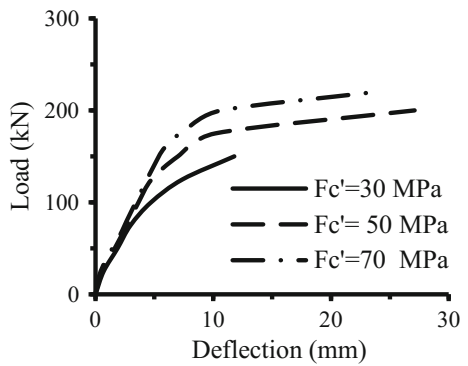


**Fig. 18** Load–deflection behavior for DT300.(#).1

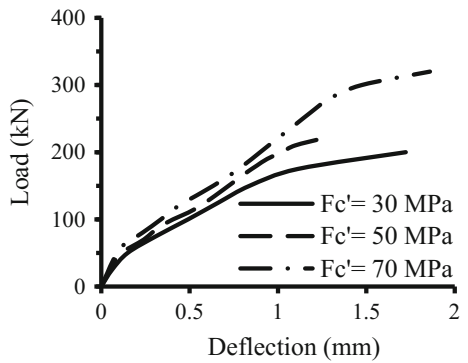


**Fig. 19** Load–deflection behavior for DT300.(#).2

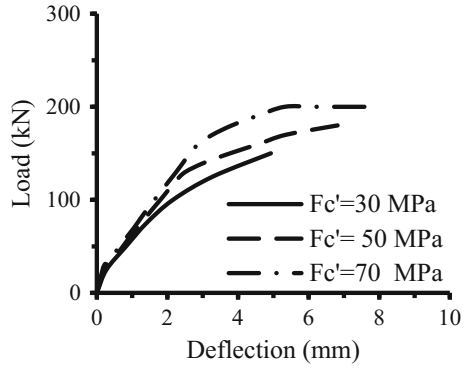


**Fig. 20** Load–deflection behavior for DT300.(#).3

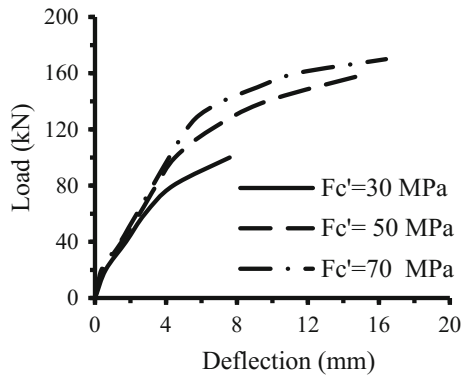


**Fig. 21** Load–deflection behavior for DT500.(#).1

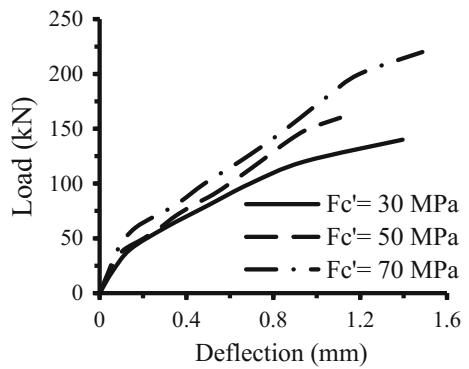


**Fig. 22** Load–deflection behavior for DT500.(#).2

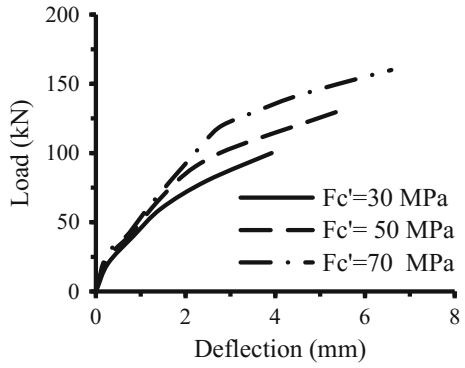


**Fig. 23** Load–deflection behavior for DT500.(#).3

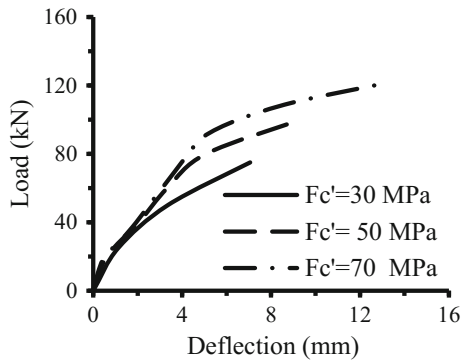
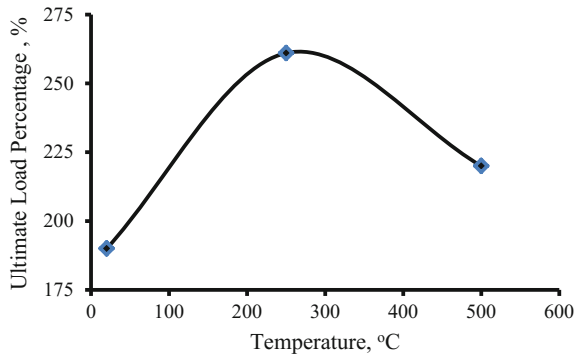


**Fig. 24** Ultimate load percentage with temperature



### 5 Effect of Length to Effective Depth Ratio ( $a/d$ )

For this study, three types of models are evaluated for analyzing the behavior of deep beams for different ( $a/d$ ) ratios. These ratios are (1, 2, and 3). Figures 25, 26, and 27, show that the load capacity decreases and deflection at failure increases with the increase in the ( $a/d$ ) ratio. This means that deep beams behave like normal beams with increasing in length. In addition, increase in midspan deflection can be noticed when the length increases [5].

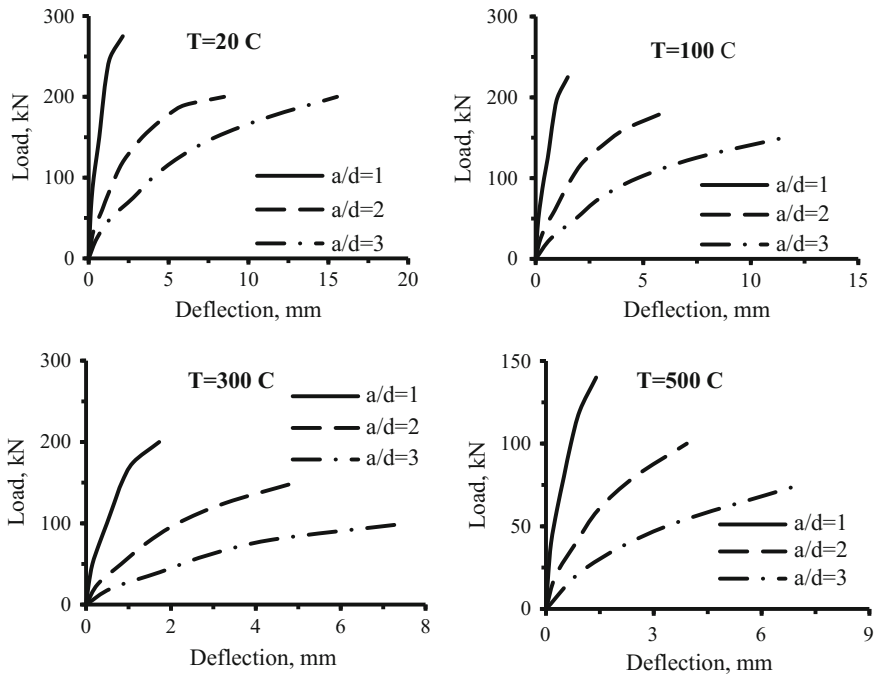


Fig. 25 Load–deflection behavior for deep beams have  $f'_c = 30$  MPa

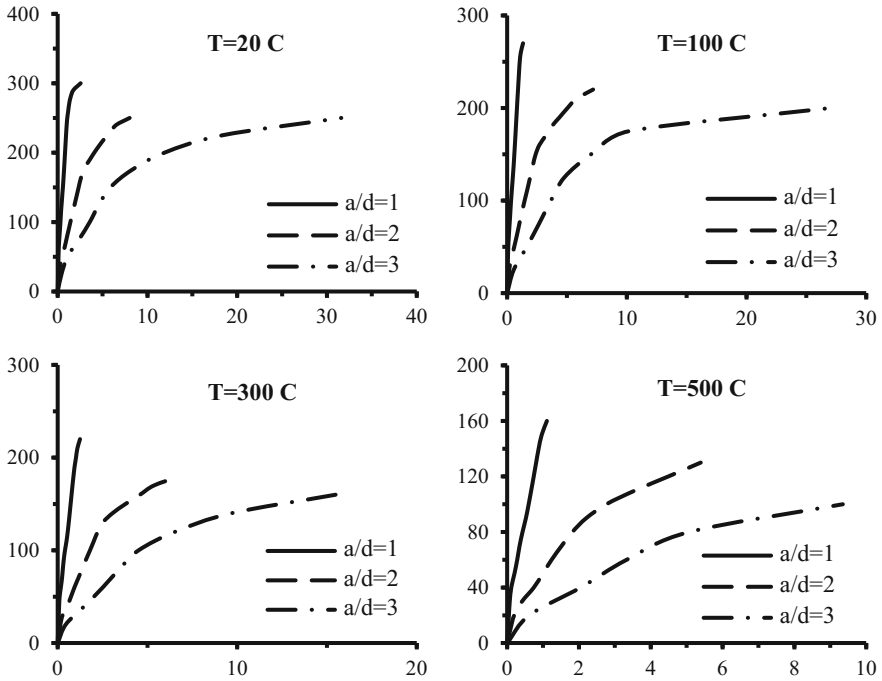


Fig. 26 Load–deflection behavior for deep beams have  $f'_c = 50$  MPa

## 6 Artificial Neural Networks by MATLAB and SPSS for the Proposed Model

### 6.1 Introduction

Due to the difficulty of analytical solutions for thermal analysis of concrete members, the results of parametric study are simulated using artificial neural networks (ANNs) to evaluate the proposed model that can be used to estimate the ultimate load of R.C. deep beams subjected to elevated temperature. The ANNs model is worked using MATLAB and SPSS facilities.

### 6.2 Neural Network by MATLAB of Proposed Model

In order to find the percentage of error and the efficiency of the proposed model, the results are divided into input matrix and output matrix, then dealing with neural network (ANN) with training (80%), testing (10%), and validation (10%). The error ( $R$ ) was (0.99) and the square value was ( $R^2 = 0.98$ ). So, the model is efficient and

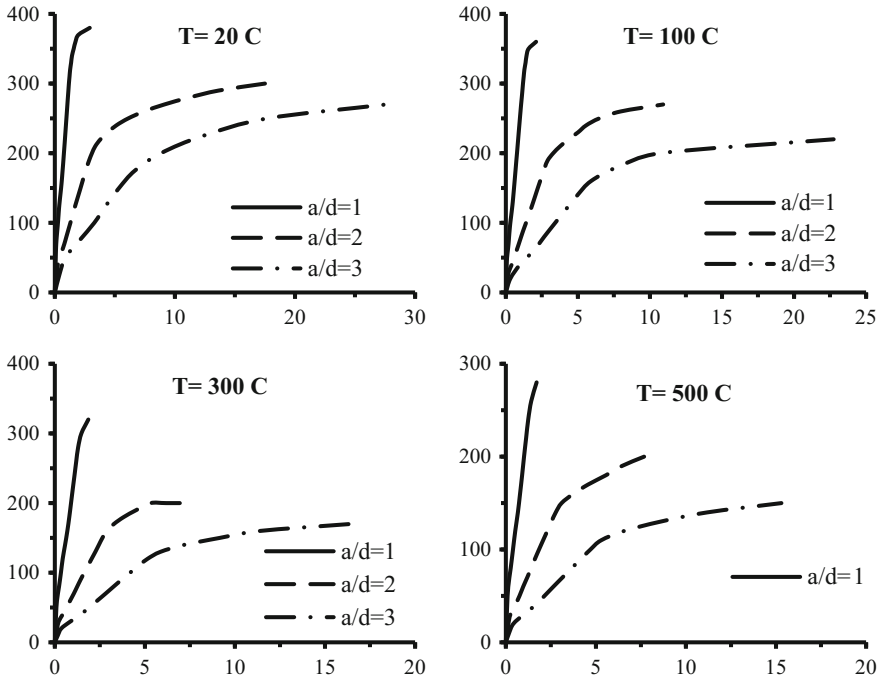


**Fig. 27** Load–deflection behavior for deep beams have  $f'_c = 70\text{ MPa}$

the error is very small. So that, the models from the parametric study can be used for making the relation curves between inputs (temperature, compressive strength, and  $a/d$  ratio) and output (ultimate load) [15–18]. Figures 28 and 29 show neural network results.

### 6.3 Proposed Model of R.C. Deep Beams Including Temperature Effect

The results of the parametric study for (105) specimens have been given as input in SPSS Skelton, eight properties that were changed in the specimens were taken and analyzed in neural networks simulations. The output window shows the results for the models with different details as well as the error percentage, and the weights (this is the most important in this study). From the weights, the equation for the ultimate load can be written. The figures show the results as shown in Tables 3, 4, 5, and 6; also, the Figs. (30, 31, and 32). All these results are illustrated and summarized the validated data for a proposed model of this study.

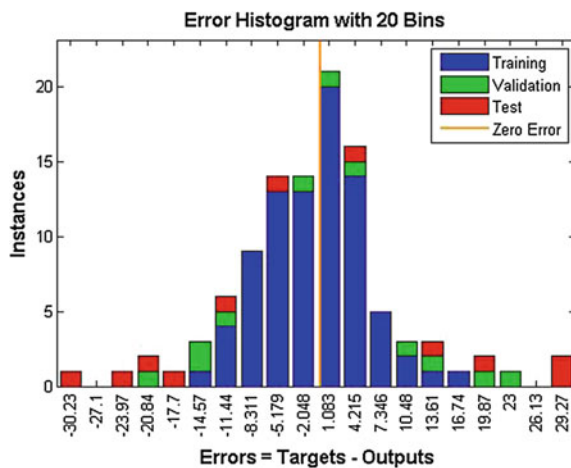


Fig. 28 Error histogram for the models

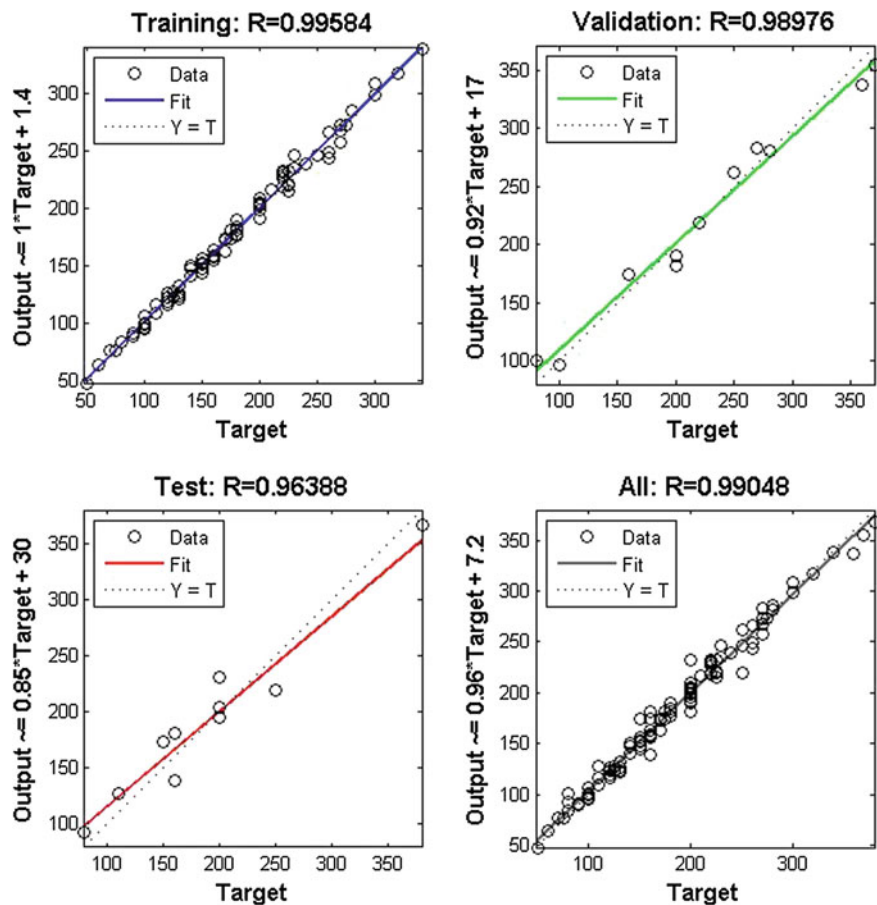


Fig. 29 Regression for the models

**Table 3** Case processing summary

		<i>N</i>	Percent
Sample	Training	78	74.3%
	Testing	17	16.2%
	Holdout	10	9.5%
Valid		105	105
Excluded		0	0
Total		105	105

**Table 4** Model summary

Training	Sum of squares error	.613
	Relative error	.073
	Stopping rule used	1 consecutive step(s) with no decrease in error <sup>a</sup>
	Training time	0:00:00.02
Testing	Sum of squares error	.106
	Relative error	.079
Holdout	Relative error	.380

Dependent variable: Pu

<sup>a</sup>Error computations are based on the testing sample

**Table 5** Independent variable importance

	Importance	Normalized importance (%)
$f_c$	.098	29.1
$E_c$	.105	31.0
$f_t$	.338	100.0
$a_d$	.107	31.8
$T$	.228	67.5
$E_{sl}$	.096	28.4
$E_{sv}$	.027	8.0

The most important result is the last figure that shows the skeleton of the modeling and the last table that shows the parameter weights that are given as input in the equation. The equation is

$$y = \frac{1}{1 + e^{-\theta_2 + w_7 \tan h(x)}} \tag{1}$$

where

$$x = \theta_1 + \sum_n^{i=1} w_i v_i \tag{2}$$



**Table 6** Parameter estimates

Predictor		Predicted	
		Hidden layer 1	Output layer
		H (1:1)	Pu
Input layer	(Bias)	.232	
	$f_c$	.172	
	$E_c$	.182	
	$f_t$	-.641	
	$a_d$	.182	
	$T$	.359	
	$E_{sl}$	.170	
	$E_{sv}$	-.042	
Hidden layer 1	(Bias)		-.004
	H (1:1)		-1.367

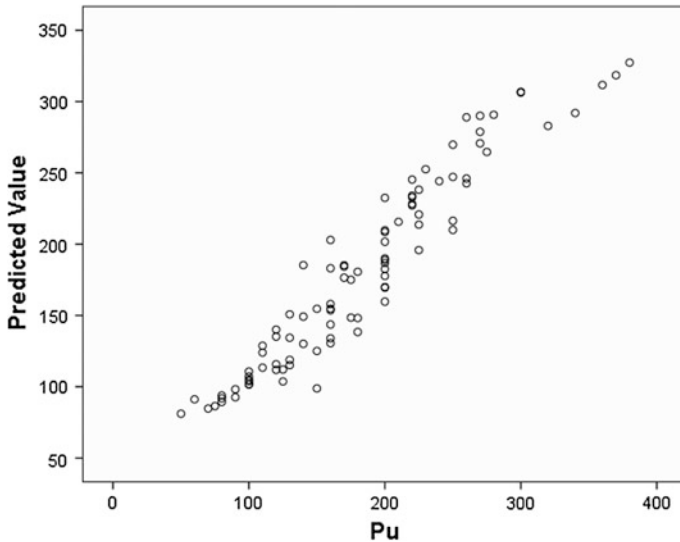


**Fig. 30** Finite element versus predicted results of max flexural capacity loads

In this study,  $x$  is

$$\begin{aligned}
 x = & 0.232 + \left(0.172 * f'_c\right) + (0.182 * E_c) - (0.641 * f_t) + \left(0.182 * \frac{a}{d}\right) \\
 & - (0.359 * T) + (0.17 * E_{sl}) - (0.042 * E_{sv})
 \end{aligned}
 \tag{3}$$

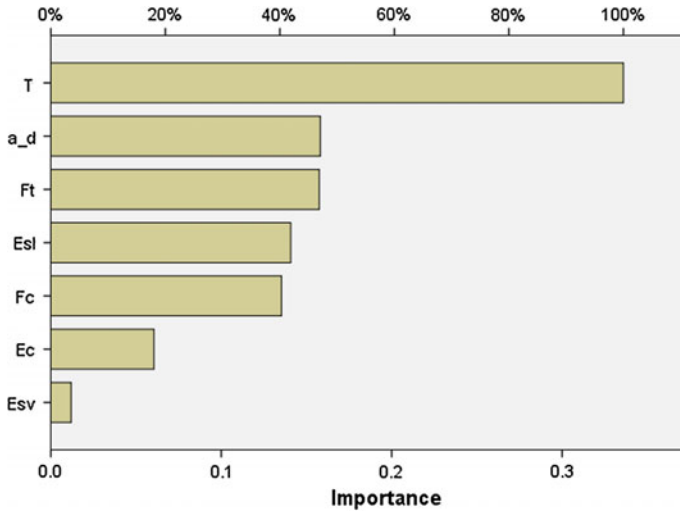


Fig. 31 Normalized importance of ANN Model

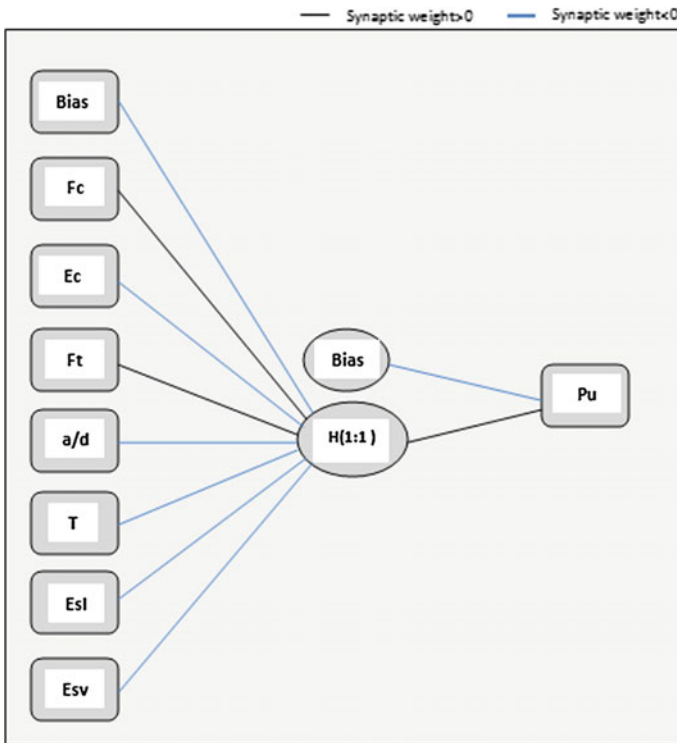


Fig. 32 The skeleton of the modeling

where

- $f_t$  splitting strength of concrete (MPa)
- $\frac{a}{d}$  effective length span-to-depth ratio
- $T$  temperature ( $^{\circ}\text{C}$ )
- $E_{sl}$  modulus of elasticity for longitudinal steel reinforcement (MPa)
- $E_{sv}$  modulus of elasticity for vertical steel reinforcement (MPa)

So Eq. (1) is

$$y = \frac{1}{1 + e^{0.004 - 1.367 \tan h(x)}} \tag{4}$$

The values of ultimate load ( $y$ ) from Eq. (4) are between (0–1) and not the real values. For getting the real values, variable weights must be corrected by using Eq. (5) as follows:

$$x = \frac{x - x_{\min}}{x_{\max} - x_{\min}} \tag{5}$$

So, the real ultimate load will be calculated from Eqs. (6) and (7) as follows:

$$y = \frac{230}{1 + e^{0.004 - 1.367 \tan h(x)}} + 50 \tag{6}$$

where  $y = P_{\text{estimate}}$ , and  $x$  is

$$\begin{aligned} x = & 0.232 + \left(0.172 * \frac{f'_c - 20}{50}\right) + \left(0.182 * \frac{E_c - 21,153}{18,421}\right) - \left(0.641 * \frac{f_t - 2.77}{2.41}\right) \\ & + \left(0.182 * \frac{\frac{a}{d} - 1}{2}\right) - \left(0.359 * \frac{T - 400}{100}\right) + \left(0.17 * \frac{E_{sl} - 117,090}{19,515}\right) - \left(0.042 * \frac{E_{sv} - 122,910}{20,485}\right) \end{aligned} \tag{7}$$

The mean absolute percentage error (MAPE) is

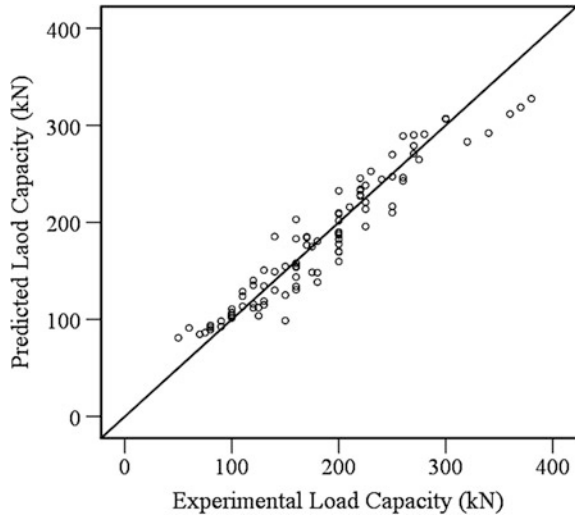
$$\text{MAPE} = \text{ABS} \left( \frac{P_{\text{actual}} - P_{\text{estimate}}}{P_{\text{actual}}} \right) \tag{8}$$

And, average accuracy percentage (AA%) is

$$\text{AA} = 100 - \text{MAPE} \tag{9}$$

The coefficient of correlation ( $R$ ) and the coefficient of determination ( $R^2$ ) are shown in Table.

**Fig. 33** Comparison between load from FEA and loads from SPSS



Name	Percentage
MAPE	76.20
AA	99.23
$R$	96.83
$R^2$	93.76

This means that the comparison between finite element models and ANN models are so good. This can be seen in Fig. 33.

## 7 Conclusions

The following conclusions are drawn based on the numerical analysis:

1. Nonlinear finite element procedure using ANSYS features to simulate reinforced concrete deep beams subjected to elevated temperature is used.
2. For checking the efficiency of the models, using neural network error  $R$  was about (99%) and square error  $R^2$  (98%).
3. The deep beam samples that have compressive strength more than 40 MPa with  $a/d = 1$ , their behavior is more distinguished when  $a/d = 2$  and  $a/d = 3$ . This means that for high-strength concrete, the effect of high temperature had less effect on concrete.
4. Deep beams having  $a/d = 1$  and temperature (20) °C, compressive strength that increase by about (3.5) times lead to increase in ultimate load about (1.9) times. But for temperature (250) °C, the ultimate load increase about (2.61) times. And for temperature (500) °C, the ultimate load increase by (2.2) times.

5. This study takes deep means for behavior of concrete with temperature changes in seasons, or in the same day between day and night, and even in the same hour between outside and inside the room if (cooling/heating) turned on. In ACI code take the large factor of error as 40%, the results from these samples exceed half of it. That makes the temperature change an important factor for concrete durability.
6. For deep beams behavior, when the length increased lead to increase in midspan deflection. And by increasing the length the deep beams behave like normal beams.

### Notations

Symbol	Descriptions
$\beta_t$	Open shear transfer coefficient
$\beta_c$	Closed shear transfer coefficient
$f'_c$	Compressive strength (MPa)
$f_y$	Yield stress (MPa)
$E$	Young's modulus (MPa)
$E_T$	Tangent modulus (MPa)
$A$	Area (mm <sup>2</sup> )
$K$	Thermal conductivity (W/m °C)
$C$	Specific heat (J/kg °C)
$\rho$	Density (kg/m <sup>3</sup> )

### References

1. ACI Committee 318: Building Code Requirements for Structural Concrete. American Concrete Institute, Farmington Hills, USA (2011)
2. ACI Committee 318M: Building Code Requirements for Structural Concrete. American Concrete Institute, Michigan, USA (2014)
3. Ama'ash, H.: New model for shear resistance of simple supported reinforced concrete deep beam. Kufa J. Eng. **3**(1) (2011) (In Arabic)
4. Chen, W.F.: Plasticity in Reinforced Concrete. McGraw-Hill, USA. [https://doi.org/10.1016/0045-7825\(82\)90016-0](https://doi.org/10.1016/0045-7825(82)90016-0)
5. Osman, B.H.: Shear in R.C. deep beams. M.Sc. thesis, University of Khartoum, Sudan (2008)
6. ANSYS, Copyright: ANSYS Help, Release 11.0. (2007)
7. Abdul Razzaq, K.S.: Effect of heating on simply supported reinforced concrete deep beams. Diyala J. Eng. Sci. **08**(02), 116–133 (2015)
8. Felicetti, R., Gambarova, P.G., Semiglia, M.: Residual capacity of HSC thermally damaged deep beams. J. Struct. Eng. **125**(3), 319–327 (1999). [https://doi.org/10.1061/\(ASCE\)0733-9445\(1999\)125:3\(319\)](https://doi.org/10.1061/(ASCE)0733-9445(1999)125:3(319))
9. American Concrete Institute: Building Code Requirements for Reinforced Concrete. Detroit, ACI-381-14 (2014)
10. Antony, N.K., Ramadass, S., Ramanujan, J.: Parametric study on the shear strength of concrete deep beam using ANSYS. Am. J. Eng. Res. (AJER) **4**, 51–59 (2013)

11. Eurocode 2: Design of Concrete Structures, Part 1-2; General Rules—Structural Fire Design. Brussels (1996)
12. European Committee for Standardisation (CEN): Eurocode 3: Design of Steel Structures, Part 1.1: General Rules and Rules for Buildings, DD ENV 1-1.EC3 (1993)
13. European Committee for Standardisation (CEN): Eurocode 4: Design of Composite Steel and Concrete Structures, Part 1.1: General Rules and Rules for Buildings, DD ENV 1-1 (1994)
14. Guo Z.: Experiment and Calculation of Reinforced Concrete at Elevated Temperatures. Tsinghua University Press. Published by Elsevier Inc., The Netherlands (2011). <https://doi.org/10.1016/c2010-0-65988-8>
15. Al-Zwainy F.M.: The use of artificial neural networks for productivity estimation of finishing stone works for building projects. *Eng. Dev. J.* **16**(2), 42–60 (2012)
16. Landau, S., Everitt, B.S.: *A Handbook of Statistical Analyses using SPSS*. Chapman & Hall/CRC Press LLC, UK (2004)
17. Mahmood A.S.: Predicting of torsional strength of prestressed concrete beams using artificial neural networks. *Int. J. Sci. Eng. Res.* **6**(2), 1222–1230 (2015)
18. Rasheed F.: Artificial neural network circuit for spectral pattern recognition. M.Sc. thesis, Texas A&M University (2013)